Online Parameter Estimation for Temporal Spectrum Sensing

Yuandao Sun, *Student Member, IEEE*, Brian L. Mark, *Senior Member, IEEE*, and Yariv Ephraim, *Fellow, IEEE*

***Abstract*—We develop a computationally efficient online parameter estimation algorithm for temporal spectrum sensing of a cognitive radio channel using a hidden bivariate Markov model. The online estimator is based on a block-recursive parameter estimation algorithm developed by Rydén for hidden Markov models. This approach requires the score function only. We develop an efficient method for computing the score function recursively and extend Rydén's approach to hidden bivariate Markov models. The advantage of the hidden bivariate Markov model over the hidden Markov model is its ability to characterize non-geometric state sojourn time distributions, which can be crucial in spectrum sensing. Based on the hidden bivariate Markov model, an estimate of the future state of the primary user can be obtained, which can be used to reduce harmful interference and improve channel utilization. Moreover, the online estimator can adapt to changes in the statistical characteristics of the primary user. We present numerical results that demonstrate the performance of temporal spectrum sensing using the proposed online parameter estimator.**

***Index Terms*—Cognitive radio, spectrum sensing, hidden Markov model (HMM), online estimation, recursive estimation.**

I. Introduction

RADIO spectrum has become an increasingly scarce communication resource due to the explosive development of wireless technologies. At the same time, spectrum measurement studies have shown that significant portions of the wireless spectrum are highly underutilized [8]. Cognitive radio enables secondary (unlicensed) users to utilize spectrum holes of primary (licensed) users, either because the primary user (PU) is idle or because the PU's location is sufficiently far from the secondary user (SU). In the first scenario, the SU performs temporal spectrum sensing to detect idle periods of the PU. In the second scenario, the SU determines the maximum transmission power that can be used in a given frequency band without causing harmful interference to PUs [16], [19], [27].

We focus here on temporal spectrum sensing for a narrowband channel. In this scenario, the PU's transmitter alternates between an active state, in which it transmits a signal onto the channel, and an idle state. A cognitive radio senses the channel by monitoring the received signal and inferring the active or idle state of the PU. Various approaches to spectrum sensing have been proposed in the literature, including matched filter detection, energy detection, and cyclostationary feature detection (cf. [34]). The matched filter detector requires prior knowledge of the modulation scheme used by the PU. Cyclostationary feature detectors perform much better under low SNR conditions, but are more computationally demanding and typically require long sensing intervals.

None of the aforementioned approaches to spectrum sensing provides the capability of forecasting the future state of the PU. By anticipating that the PU will change from the idle to the active state, a cognitive radio could vacate the channel well before such an event occurred, thereby reducing the potential interference to the PU. In [24], an approach to model-based temporal spectrum sensing was proposed based on a hidden bivariate Markov model (HBMM). In this context, the HBMM consists of an underlying bivariate Markov chain, which models the state sequence of the PU (i.e., active or idle), together with an observation model, which characterizes the lognormal shadow fading of the channel between the PU and the cognitive radio. Forward recursions developed in [24] are used to compute estimates of the current state of the PU, as well as predicted estimates of futures states. The HBMM is closely related to the more familiar hidden Markov model (HMM) (cf. [7]). A key benefit of the HBMM for the spectrum sensing application is that the sojourn times of the PU in the active and idle states could be modeled by discrete phase-type distributions, whereas in an HMM the model for sojourn times is limited to geometric distributions. The ability of the HBMM to characterize general state sojourn times is important for accurate prediction of the future state of a PU.

In the temporal spectrum sensing scheme proposed in [24], the Baum algorithm [2] is applied to training data to estimate the HBMM parameter. The HBMM parameter estimate is then used to perform state estimation and prediction via forward recursions. This approach was shown to perform well on real spectrum measurement data with respect to estimation and prediction error probabilities. Due to the offline nature of the Baum algorithm, however, it cannot adapt to changes over time in the wireless channel or in the underlying statistics of the PU transmission pattern.

In this paper, we develop an online parameter estimation scheme for the HBMM and apply it to temporal spectrum sensing. The estimation and prediction accuracy of this scheme is comparable to that of the offline Baum-based parameter estimator in [24]. Since the estimator is recursive, it is able to adapt to slow changes in the statistical behavior of the PU's

Manuscript received June 17, 2014; revised November 7, 2014 and January 22, 2015; accepted March 9, 2015. Date of publication March 26, 2015; date of current version August 10, 2015. This work was supported in part by the U.S. National Science Foundation under Grants CCF-0916568, CNS-1205453, and CNS-1421869. The associate editor coordinating the review of this paper and approving it for publication was Z. Wang.

The authors are with the Department of Electrical and Computer Engineering, George Mason University, Fairfax, VA 22030 USA (e-mail: ysun12@gmu.edu; bmark@gmu.edu; yephraim@gmu.edu).

Color versions of one or more of the figures in this paper are available online at http://ieeexplore.ieee.org.

Digital Object Identifier 10.1109/TWC.2015.2416720

transmission pattern. The operational assumption here is that the state sequence representing the PU active/idle intervals is quasi-stationary. That is, the sequence may be conceptually divided into segments such that each segment is drawn from a possibly different stationary sequence. The proposed online HBMM parameter estimator is based on a block-recursive parameter estimation scheme originally developed by Rydén for HMMs [25]. We adopt a method due to Willy *et al.* [32] to estimate the score function of the HBMM. Together with the state estimation and prediction recursions presented in [24], the HBMM parameter estimator forms the basis for a fully online scheme for temporal spectrum sensing.

Much of the prior work on model-based temporal spectrum sensing relies on the more traditional univariate Markov chain, either in discrete-time or continuous-time, to model the PU. Several papers have used the standard HMM to jointly model the PU state and the effect of the channel. A recent paper by Li *et al.* [17], develops a sequential particle filtering approach for joint estimation of the current state of the PU and of the channel. In [17], a two-state discrete-time Markov chain model for the PU is assumed and the channel is modeled by a finite state Markov chain to characterize time-variant small-scale fading. Empirical results presented in [9], [24] provide evidence of the non-geometric nature of the active and idle periods of a PU. In [9], a continuous-time semi-Markov process was proposed as a model for the PU. Unlike the hidden semi-Markov model [33], the HBMM does not require explicit specification or estimation of the state sojourn time distributions. We mention that the HBMM and related models have been applied in other applications, such as unsupervised image segmentation (see, e.g., [14]).

The remainder of the paper is organized as follows. In Section II, temporal spectrum sensing based on the HBMM is discussed. In Section III, we develop an online parameter estimation algorithm for HBMMs and discuss its application to spectrum sensing. In Section IV, we present numerical results to demonstrate the performance of the proposed online spectrum sensing scheme. In Section V, we provide some concluding remarks.

II. Spectrum Sensing Based on a Hidden Bivariate Markov Model

In this section, we briefly review the framework for spectrum sensing proposed in [24], focusing on the role of the HBMM and estimation of the HBMM parameter.

A. System Model

The PU alternates between an active state, in which a signal of fixed output power is transmitted over a narrowband channel and an idle state, in which no signal is transmitted. The wireless propagation environment is assumed to be governed by a standard path loss with lognormal shadowing model. For a receiver at a distance δ from the PU, the overall log-distance path loss with shadowing, measured in dB, is given by [20, pp. 40–41]

$$L_p(\delta) = \bar{L}_p(\delta_0) + 10\kappa \log_{10}\left(\frac{\delta}{\delta_0}\right) + \epsilon_{\mathrm{dB}}, \quad \delta \geq \delta_0, \qquad (1)$$

where δ_0 denotes the close-in reference distance, $\bar{L}_p(\delta_0)$ is the average log-distance path loss at the reference distance δ_0, κ is the path loss exponent, and ϵ_{dB} is the shadowing noise, which is assumed to be a Gaussian random variable with zero mean and variance σ_ϵ^2. We ignore fast fading since it can be reduced effectively by an averaging filter (cf. [18]).

We shall assume a discrete-time model. Let Y_k denote the received signal power at time k from the PU, measured in units of dBm, by the cognitive radio. Let X_k denote the transmission state of the PU at time k. We use $X_k = 1$ to signify the idle state, i.e., no transmission by the PU and $X_k = 2$ to indicate the active state, i.e., transmission by the PU. Under the path loss model in (1), Y_k depends on X_k as follows:

$$Y_k = \begin{cases} \mu_1 + \epsilon_{1,\mathrm{dB}}, & X_k = 1, \\ \mu_2 + \epsilon_{2,\mathrm{dB}}, & X_k = 2, \end{cases} \qquad (2)$$

where μ_a represents the mean received signal power in dBm and $\epsilon_{a,\mathrm{dB}}$ is a zero-mean Gaussian random variable with variance σ_a^2 representing the associated shadowing noise, when the transmission state of the PU is $a \in \{1, 2\}$. The signal power μ_a results from the transmit power in state a and the path loss from transmitter to receiver, as expressed in the deterministic part of (1).

Typically, the sequence Y of received signal powers undergoes pre-processing at the front-end of the receiver. For example, usually some form of averaging is applied to the received signal power samples to diminish the effect of fast fading in the wireless propagation environment (cf. [18]). After applying averaging, the front-end becomes essentially the same as that of a classical energy detector. With a slight abuse of notation, we shall refer to the output of the receiver front-end as $Y = \{Y_k\}_{k=1}^{\infty}$. In this case, the form of relation (2) remains valid, i.e., Y is conditionally Gaussian given X.

B. Hidden Bivariate Markov Model

In the literature on spectrum sensing, the PU state sequence X is commonly assumed to be a Markov chain (cf. [1], [9]–[11], [23], [28]). In this case, the joint process (Y, X) is an HMM (see, e.g., [7] for a review of HMMs). HMMs have been applied as models for a cognitive radio channel in several papers, e.g., [1], [11], [23], [28]. A limitation of the HMM, however, is that the Markov assumption on the state sequence X restricts the sojourn time in a given state to be geometrically distributed. On the other hand, empirical studies have shown that the state sojourn time distributions are often not adequately characterized by geometric distributions. For example, in [9], a continuous-time semi-Markov process was proposed as a model for the state process, while in [29], source traffic models with lognormal and extreme value sojourn time distributions were studied.

The HBMM adopted in this paper is a trivariate process (Y, X, S), where Y denotes an observable process with continuous alphabet and the underlying sequence, $Z = (X, S)$, is a finite state bivariate Markov chain. In this setup, the auxiliary process S, together with the PU state process X, form a Markov chain, such that X alone is not Markov, and consequently, its

sojourn time in each state has a phase-type distribution. Such distribution is far more general than the geometric distribution of the HMM, as we elaborate below. For a general HBMM, we denote the state-space of X by $\mathbb{X} = \{1, \ldots, d\}$ and the state-space of S by $\mathbb{S} = \{1, \ldots, r\}$. The state-space of Z is given by $\mathbb{Z} = \mathbb{X} \times \mathbb{S}$. The processes Y and S are assumed to be conditionally independent given X. In addition, Y given X is a sequence of independent, identically distributed (iid) random variables.

Let $f(y; \theta_a)$ denote the conditional density of Y_k given $X_k = a$, where θ_a is a parameter depending on $a \in \mathbb{X}$. In the spectrum sensing application, the form of $f(y; \theta_a)$ depends on the particular channel model and receiver front-end assumed. Under the setup of (2), $f(y; \theta_a)$ is a Gaussian density and in this case, we set $\theta_a = (\mu_a, \sigma_a)$, where μ_a and σ_a denote the mean and standard deviation in state a. The d-tuple $\theta = (\theta_a : a \in \mathbb{X})$ specifies the conditional Gaussian parameters of the HBMM. Different channel models and receiver front-ends could be accommodated within the HBMM framework by modifying the form of $f(y; \theta_a)$ appropriately. We remark that the assumption that Y is conditionally independent given X could be relaxed by characterizing the observable process as a vector process $\boldsymbol{Y} = \{\mathbf{Y}_n\}$, where the random vector $\mathbf{Y}_n$ captures correlations among consecutive components of the process Y. For example, to capture pairwise correlations in the observable process, one could define $\mathbf{Y}_n = (Y_{2n-1}, Y_{2n}),\ n = 1, 2, \ldots$. Nevertheless, the simple Gaussian-based HBMM was found to be quite accurate in modeling real spectrum measurement data [22], [24].

Let P denote the underlying probability measure. The initial distribution of the bivariate Markov chain Z is denoted by the $1 \times dr$ row vector $\pi = [\pi_{(a,i)} : (a, i) \in \mathbb{Z}]$, where $\pi_{(a,i)} = P(Z_1 = (a, i))$, and lexicographic ordering of the bivariate states is assumed. The transition probability matrix of Z is denoted by the $dr \times dr$ matrix $G = [g_{ab}(ij) : (a, i), (b, j) \in \mathbb{Z}]$, where $g_{ab}(ij) = P(Z_2 = (b, j) | Z_1 = (a, i))$. The transition matrix can be expressed as a block matrix $G = [G_{ab} : a, b \in \mathbb{X}]$, where $G_{ab} = [g_{ab}(i, j) : i, j \in \mathbb{S}]$ is an $r \times r$ matrix. We assume that the matrices G and G_{aa}, $a \in \mathbb{X}$, are irreducible and that the diagonal elements of G are positive.

Statistical properties of discrete-time bivariate Markov chains are discussed in [5, Chapter 8], [24]. In particular, the sojourn time of the process X in each state $a \in \mathbb{X}$ has a discrete-time phase-type distribution. Suppose that X jumps at some time k. Let ζ_a denote the conditional distribution of S_k given that $X_k = a$. Then the probability mass function of the sojourn time of X in state a is given by

$$p(t \mid a) = \zeta_a G_{aa}^{t-1} (I - G_{aa}) \mathbf{1}, \quad t = 1, 2, \ldots, \tag{3}$$

where $\mathbf{1}$ denotes a column vector of all ones and I denotes an identity matrix of a given dimension. This is a discrete phase-type distribution with parameter (ζ_a, G_{aa}) [21, p. 46]. The family of phase-type distributions is dense in the set of distributions on $\{0, 1, 2, \ldots\}$ [15, p. 54] and includes convolutions as well as mixtures of geometric distributions. Thus, a phase-type distribution can approximate any given state sojourn time distribution arbitrarily closely. Increasing the number of states of the process S allows more degrees of freedom in the phase-type sojourn time distribution.

The parameter of the HBMM is specified by $\phi = (\pi, \theta, G)$. We note that the number of elements in the parameter ϕ could be reduced, since each row of G sums to one. However, there is a practical benefit to retaining the entire matrix G as part of the HBMM parameter (see Section IV-A). When an HMM (Y, X) is used instead of the HBMM, Y given X is assumed to have the same distribution as in the HBMM. The initial distribution π is given by the $1 \times d$ vector $\pi = [\pi_a : a \in \mathbb{X}]$ with $\pi_a = P(X_1 = a)$, and the transition matrix G is given by $G = [g_{ab} : a, b \in \mathbb{X}]$, where $g_{ab} = P(X_2 = b | X_1 = a)$. Clearly, the HMM parameter represents a special HBMM for which $r = 1$.

C. State and Parameter Estimation

In the spectrum sensing approach developed in [24], a training sequence of signal strength measurements from a cognitive radio channel is used to estimate the parameter of an HBMM in the maximum likelihood sense using a batch expectation-maximization algorithm [3], which is essentially the Baum algorithm [2]. The Baum algorithm involves both forward and backward recursions and iterates over a given sequence of observations. Given an HBMM parameter estimate, $\hat{\phi}$, forward recursions can be used to estimate the current state and predict a future state of the PU, given the current and past observation data. In Section III, we develop a block-recursive online algorithm, which updates the HBMM parameter estimate after every m samples, where m denotes the block size. To perform state estimation and prediction in conjunction with the online parameter estimator, the same forward recursions developed in [24] can be applied, except that the HBMM parameter used in the recursions is dynamic, rather than static. This results in a fully online approach to temporal sensing, which does not require a training phase.

We next provide a brief outline of the state estimation and prediction scheme developed in [24]. To simplify notation, given a sequence $\{y_k\}$, we denote a subsequence $\{y_k, \ldots, y_n\}$, $k \le n$, by y_k^n. When $k = 1$, we denote the subsequence y_1^n simply by y^n. Given an HBMM parameter ϕ, the conditional probability of the bivariate state Z_k given y^k, denoted by $p_\phi(z_k | y^k)$, follows straightforwardly from the forward recursion for an HMM, (see, e.g., [24, Eq. (14)]). For an integer $\tau \ge 0$, the conditional probability of the bivariate state $Z_{k+\tau}$ given y^k is obtained from (see, e.g., [24, Eq. (22)])

$$\begin{aligned} p_\phi(z_{k+\tau} \mid y^k) &= \sum_{z_k \in \mathbb{Z}} p_\phi(z_k \mid y^k)\, p_\phi(z_{k+\tau} \mid z_k) \\ &= \sum_{z_k \in \mathbb{Z}} \bar{\alpha}(z_k, y^k) [G^\tau]_{z_k, z_{k+\tau}}, \end{aligned} \tag{4}$$

where $\bar{\alpha}(z_k, y^k) = p_\phi(z_k | y^k)$ is computed using the scaled forward recursion for an HMM. Define a $dr \times dr$ block diagonal matrix $B(y_k)$, with its diagonal blocks given by $\{p(y_k | X_k = a) I, a \in \mathbb{X}\}$, for $k = 1, 2, \ldots$. The scaled forward recursion is given by (cf. [24, Eq. (14)])

$$\bar{\alpha}_1 = \frac{\pi B(y_1)}{c_1},\ \bar{\alpha}_k = \frac{\bar{\alpha}_{k-1} G B(y_k)}{c_k},\ k = 2, 3, \ldots, \tag{5}$$

where $c_1 = \pi B(y_1) \mathbf{1}$, and $c_k = \bar{\alpha}_{k-1} G B(y_k) \mathbf{1}$.

A detection scheme for the state of the PU at time $k+\tau$ given the observation sequence y^k is specified as follows (cf. [24, Eq. (23)]):

$$\hat{X}_{k+\tau|k} = \begin{cases} 1, & \text{if } \sum_{s_{k+\tau}\in\mathbb{S}} p_\phi(z_{k+\tau} = (1, s_{k+\tau})|\, y^k) \geq \eta, \\ 2, & \text{otherwise,} \end{cases} \tag{6}$$

for $k = 1, 2, \ldots$, where η is a decision threshold, $0 < \eta < 1$. The detection scheme is a maximum a posteriori (MAP) detector when $\eta = 0.5$. When $\tau = 0$, $\hat{X}_{k+\tau|k} = \hat{X}_{k|k}$ is an estimate of the current state X_k. When $\tau = 1, 2, \ldots$, $\hat{X}_{k+\tau|k}$ is the τ-step predicted estimate of the state $X_{k+\tau}$. The current and predicted state estimates $\hat{X}_{k+\tau|k}$ can be directly applied to make dynamic spectrum access decisions.

The main thrust of the present paper lies in developing an online algorithm to update the parameter estimate used in (6) at regular intervals. A fully online temporal spectrum sensing is obtained by executing (6) at each time step k with ϕ replaced by the most recent HBMM parameter estimate $\hat{\phi}_n$ computed by the online parameter estimator given by (8) in Section III. The state estimation/prediction scheme (6) and the online parameter estimator (8) run in parallel. To quantitatively assess the performance of the online temporal spectrum sensing scheme, a receiver operating characteristic (ROC) curve can be obtained by determining the false alarm and missed detection probabilities for the scheme (6) corresponding to each value of η in the interval (0,1). Examples of such ROC curves are presented in Section IV.

III. Online Parameter Estimation Algorithm

In this section, we develop an efficient online parameter estimation algorithm for the HBMM. The algorithm extends an earlier online algorithm developed by Rydén for HMMs [25]. Other recursive parameter estimation schemes for HMMs have been proposed in the literature, notably the schemes proposed by Holst and Lindgren [12] and Krishnamurthy and Moore [13]. In contrast to these schemes, Rydén's algorithm is block-recursive and has lower computational complexity, as it does not involve scaling matrices. Moreover, numerical results presented in [25] show that estimates obtained using Rydén's scheme had much smaller variances than those obtained via the Holst-Lindgren procedure.

A. Rydén's Block-Recursive Estimator for HMMs

Consider an HMM (Y, X), where X is a time-homogeneous Markov chain with state-space $\mathbb{X} = \{1, \ldots, d\}$ and Y is a sequence of conditionally independent random variables given X. In practice, the effect of the initial probability distribution π on the Markov chain quickly fades and accurate estimation of π is not necessary. Therefore, we parametrize the HMM by the row vector $\phi = [\mu_a, \sigma_a, g_{ab} : a, b \in \mathbb{X}]$. The total number of elements in ϕ is given by $L = 2d + d^2$, so we may write $\phi = [\phi_\ell : \ell = 1, \ldots, L]$. We also denote the space of HMM parameters by $\Phi \subseteq \mathbb{R}^L$.

Rydén's algorithm operates on a block of observation data at a time. Let m denote the block size and let

$$\chi(y^m; \phi) = \frac{\partial \log p_\phi(y^m)}{\partial \phi} \tag{7}$$

be the score function associated with the joint density of Y^m under the parameter ϕ, denoted by $p_\phi(y^m)$. Here, χ is the $1 \times L$ gradient row vector of $\log p_\phi(y^m)$ with respect to ϕ. Rydén's recursive parameter estimator is based on a stochastic approximation algorithm of the following form:

$$\hat{\phi}_{n+1} = \Pi_{\mathcal{G}} \left[\hat{\phi}_n + \gamma_n \chi \left(y_{nm+1}^{(n+1)m}; \hat{\phi}_n \right) \right], \tag{8}$$

where $\Pi_{\mathcal{G}}$ denotes a projection operator, which is a mapping into a compact, convex set $\mathcal{G} \subseteq \Phi$. In the recursion (8), $\hat{\phi}_{n+1}$ is the $(n+1)$-st estimate of the HMM parameter, computed as a function of the observation samples $y_{nm+1}, \ldots, y_{(n+1)m}$ and the nth estimate $\hat{\phi}_n$. The sequence $\{\gamma_n\}$ is defined by $\gamma_n = \gamma_0 n^{-\varepsilon}$ for some $\gamma_0 > 0$ and $\varepsilon \in \left(\frac{1}{2}, 1\right]$. Under some mild assumptions, Rydén proved that the sequence $\{\hat{\phi}_n\}$ converges to a point lying in the set of Kuhn-Tucker points for minimizing the Kullback-Leibler divergence defined over $\mathcal{G}$. Assuming that the estimator (8) is consistent, it converges at a rate $n^{-\alpha/2}$ with $\alpha < 1$. Under some additional, relatively mild assumptions, Rydén showed that the averaged estimator

$$\bar{\phi}_n = \frac{1}{n} \sum_{k=1}^{n} \hat{\phi}_k \tag{9}$$

converges at rate $n^{-1/2}$ and is asymptotically normal. For convenience, we will simply refer to (8) as the online parameter estimator, with the understanding that the estimates $\hat{\phi}_n$ are averaged according to (9).

In practice, convergence of a parameter estimator could be measured in terms of a relative distance between consecutive parameter estimates, since the value of the true parameter is unknown. For example, one could use

$$\frac{\|\hat{\phi}_{n-1} - \hat{\phi}_n\|}{\|\hat{\phi}_n\|} < \omega_{th}, \tag{10}$$

where $\|\cdot\|$ denotes a norm and ω_{th} is an appropriate threshold. For comparison, we note that convergence of the batch Baum algorithm could be assessed through a relative distance between consecutive values of the likelihood function, which is readily available. Such likelihood function is not available for the online algorithm.

B. Online Parameter Estimator for HBMM

We next extend Rydén's algorithm by deriving a recursive procedure for computing the score function of an HBMM (Y, X, S), based on the approach of Willy *et al.* [32], which was originally developed for MMPPs. This results in an online parameter estimator for the HBMM. We remark that the theoretical convergence results established by Rydén for his recursive parameter estimation algorithm for the HMM carry over to the HBMM case, since an HBMM (Y, X, S), as defined in Section II, is mathematically equivalent to an HMM (Y, U), where U is a univariate Markov chain with state space $\mathbb{U}$ isomorphic to $\mathbb{Z} = \mathbb{X} \times \mathbb{S}$. In spite of this mathematical equivalence, the specific details of the application of the HBMM yield the desired sojourn time phase-type distribution for this model, which is the primary advantage of the HBMM compared to the HMM.

The HBMM is parametrized by

$$\phi = [\mu_a,\ \sigma_a,\ g_{ab}(ij) :\ (a,i),(b,j) \in \mathbb{Z}].$$

We also denote the parameter by $\phi = [\phi_\ell : \ell = 1, \ldots, L]$, with $L = 2d + d^2r^2$. The score function for the observed sequence y^m is the $1 \times L$ row vector given by

$$\begin{aligned}\chi(y^m;\phi) &= \frac{1}{p_\phi(y^m)} \frac{\partial}{\partial \phi} p_\phi(y^m) \\ &= \sum_{(b,j)\in\mathbb{Z}} \frac{1}{p_\phi(y^m)} \frac{\partial}{\partial \phi} p_\phi\left(y^m, z_m = (b,j)\right). \quad (11)\end{aligned}$$

Let $H_m(y^m;\phi)$ denote a $dr \times L$ matrix whose (v,ℓ) element is given by

$$[H_m(y^m;\phi)]_{v\ell} = \frac{1}{p_\phi(y^m)} \frac{\partial}{\partial \phi_\ell} p_\phi\left(y^m, z_m = (b,j)\right), \quad (12)$$

where $(b,j) \in \mathbb{Z}$ such that $v = b(r-1) + j$ and $l \in \{1, \ldots, L\}$. Then the score function can be obtained from

$$\chi(y^m;\phi) = \mathbf{1}' H_m(y^m;\phi), \quad (13)$$

where $'$ denotes matrix transpose. Applying the conditional independence of the observation sequence Y given the underlying Markov chain Z yields $[H_m(y^m;\phi)]_{v\ell}$ as

$$\begin{aligned}&\frac{1}{p_\phi(y^m)} \frac{\partial}{\partial \phi_\ell} \sum_{(a,i)\in\mathbb{Z}} p_\phi\left(y^{m-1}, z_{m-1} = (a,i)\right) f_{ij}^{ab}(y_m;\theta_b) \\ &= \frac{1}{p_\phi(y_m \mid y^{m-1})} \sum_{(a,i)\in\mathbb{Z}} \frac{1}{p_\phi(y^{m-1})} \\ &\quad \cdot \frac{\partial}{\partial \phi_\ell} \left[p_\phi\left(y^{m-1}, z_{m-1} = (a,i)\right) f_{ij}^{ab}(y_m;\theta_b)\right], \quad (14)\end{aligned}$$

where $f_{ij}^{ab}(y_m;\theta_b) \triangleq g_{ab}(ij) f(y_m;\theta_b)$. Comparing (12) and (14), a recursive procedure for computing $H_m(y^m;\phi)$ can be obtained as follows:

$$\begin{aligned}[H_m(y^m;\phi)]_{v\ell} = \frac{1}{c_m} \sum_{(a,i)\in\mathbb{Z}} \Big\{ &\left[H_{m-1}(y^{m-1};\phi)\right]_{u\ell} \\ &\cdot f_{ij}^{ab}(y_m;\theta_b) + \xi_{m-1}(a,i) \frac{\partial}{\partial \phi_\ell} f_{ij}^{ab}(y_m;\theta_b) \Big\}, \quad (15)\end{aligned}$$

where $u = a(r-1) + i$ and

$$\begin{aligned}\xi_m(b,j) &\triangleq p_\phi(z_m = (b,j) \mid y^m) \\ &= \frac{1}{c_m} \sum_{(a,i)\in\mathbb{Z}} \xi_{m-1}(a,i) f_{ij}^{ab}(y_m;\theta_b), \quad (16) \\ c_m &\triangleq p_\phi(y_m \mid y^{m-1}) \\ &= \sum_{(a,i)\in\mathbb{Z}} \sum_{(b,j)\in\mathbb{Z}} \xi_{m-1}(a,i) f_{ij}^{ab}(y_m;\theta_b). \quad (17)\end{aligned}$$

Let ξ_m be a $1 \times dr$ row vector given by

$$\xi_m = [\xi_m(a,i) : (a,i) \in \mathbb{Z}] \quad (18)$$

and define a $dr \times dr$ matrix

$$F(y_m) = \left[f_{ij}^{ab}(y_m;\theta_b) : (a,i),(b,j) \in \mathbb{Z}\right]. \quad (19)$$

Then (16) and (17) can be expressed more compactly as

$$\xi_m = \frac{1}{c_m} \xi_{m-1} F(y_m), \quad (20)$$

and

$$c_m = \xi_{m-1} F(y_m) \mathbf{1}, \quad (21)$$

respectively. Equation (15) can then be expressed in matrix form as follows:

$$\begin{aligned}H_m(y^m;\phi) = \frac{1}{c_m} \Big\{ &F(y_m)' H_{m-1}(y^{m-1};\phi) \\ &+ (I \otimes \xi_{m-1}) \frac{\partial}{\partial \phi} \left[\text{vec } F(y_m)\right]' \Big\}, \quad (22)\end{aligned}$$

where I denotes an identity matrix, of order dr in this case, $\otimes$ denotes the Kronecker product, and $\text{vec}F(y_m)$ denotes the $d^2r^2 \times 1$ column vector obtained by stacking the columns of the matrix $F(y_m)$ one on top of the other. The form of (22) is particularly convenient for implementing the online parameter estimator in a vector-based programming language such as MATLAB. The $d^2r^2 \times L$ matrix $\partial[\text{vec } F(y_m)]'/\partial\phi$ is the Jacobian of the vector-valued function $[\text{vec } F(y_m)]'$ with respect to the HBMM parameter ϕ. The elements of the $d^2r^2 \times L$ Jacobian matrix $\partial[\text{vec } F(y_m)]'/\partial\phi$ are partial derivatives of $f_{ij}^{ab}(y_m;\theta_b)$, given as follows:

$$\begin{aligned}\frac{\partial f_{ij}^{ab}(y_m;\theta_b)}{\partial [g_{ce}(\iota l)]} &= f(y_m;\theta_b) \mathbf{1}_{\{(c,\iota)=(a,i),(e,l)=(b,j)\}}, \\ \frac{\partial f_{ij}^{ab}(y_m;\theta_b)}{\partial (\sigma_c)} &= f_{ij}^{ab}(y_m;\theta_b) \frac{(y_m - \mu_b)^2 - \sigma_b^2}{\sigma_b^3} \mathbf{1}_{\{c=b\}}, \\ \frac{\partial f_{ij}^{ab}(y_m;\theta_b)}{\partial (\mu_c)} &= f_{ij}^{ab}(y_m;\theta_b) \frac{y_m - \mu_b}{\sigma_b^2} \mathbf{1}_{\{c=b\}},\end{aligned}$$

for $(c,\iota),(e,l) \in \mathbb{Z}$, where $\mathbf{1}_A$ denotes an indicator function on the set A.

The computational complexity of the online estimator at each step is dominated by the computation of the matrix $H_m(y^m;\phi)$ in (22), which requires $O((d^3r^3)L) = O(d^5r^5)$ arithmetic operations for the HBMM, assuming a straightforward sequential implementation. For the spectrum sensing application, $d = 2$, so the complexity of the estimator grows as $O(r^5)$. In practice, a larger value of r can yield more accurate parameter estimates, but then more observation data would be required for the estimator to converge. In our numerical experiments, we have used values of r ranging from 1 to 5. We remark that each iteration of the Baum algorithm proposed in [24] has computational complexity $O(r^2T)$, where T is the length of the observation sequence used to compute the estimate and is typically quite large (e.g., $T = 2000$). Furthermore, the Baum algorithm may require many iterations to converge.

IV. Numerical Results

In this section, we presents the results of a numerical study to assess the accuracy of the proposed algorithm in estimating the parameter of an HBMM and in estimating the state of the PU for online spectrum sensing.

A. Implementation

The online HBMM parameter estimator was implemented in MATLAB. The block size is chosen to be $m = 20$ and the averaging procedure (9) is started after the basic recursion (8) has been executed for 1,000 steps. For the projection step in (8), we define the parameter space $\mathcal{G}$ as follows:

$$\mathcal{G} = \Bigg\{ \phi : \mu_a \in (\underline{\mu}, \bar{\mu}), \sigma_a \in (0, \bar{\sigma}), g_{ab}(ij) \in (\underline{g}, \bar{g}), \sum_{(b,j)\in\mathbb{Z}} g_{ab}(ij) = 1; (a,i),(b,j) \in \mathbb{Z} \Bigg\},$$

where $\underline{\mu} = -10^6$, $\bar{\mu} = 10^6$, $\bar{\sigma} = 100$, $\underline{g} = 10^{-6}$, and $\bar{g} = 1 - 10^{-6}$. The projection operator $\Pi_{\mathcal{G}}$ in (8) can be implemented in various ways. We have obtained good results using the following approach. Let $\tilde{\phi}$ denote the bracketed expression in (8). Recall that the parameter ϕ is the triplet $[\mu, \sigma, G]$. The components of $\hat{\phi}_{n+1}$ are obtained from the corresponding components of $\tilde{\phi}$ using

$$\hat{\mu}_a^{(n+1)} = \begin{cases} \tilde{\mu}_a, & \tilde{\mu}_a \in (\underline{\mu}, \bar{\mu}), \\ \hat{\mu}^{(n)}, & \text{otherwise}, \end{cases}$$

$$\hat{\sigma}_a^{(n+1)} = \begin{cases} \tilde{\sigma}_a, & \tilde{\sigma}_a \in (\underline{\sigma}, \bar{\sigma}), \\ \hat{\sigma}^{(n)}, & \text{otherwise}, \end{cases}$$

for $a \in \mathbb{X}$ and

$$\hat{g}_{ab}^{(n+1)}(ij) = \frac{\hat{g}_{ab}(ij)}{\sum_{(b,j)\in\mathbb{Z}} \hat{g}_{ab}(ij)}, \tag{23}$$

where

$$\hat{g}_{ab}(ij) = \begin{cases} \hat{g}_{ab}^{(n)}(ij)\Big(1 + \tilde{g}_{ab}(ij) - \hat{g}_{ab}^{(n)}(ij)\Big), & \tilde{g}_{ab}(ij) \in (\underline{g}, \bar{g}), \\ \hat{g}_{ab}^{(n)}(ij), & \text{otherwise}, \end{cases} \tag{24}$$

for $(a,i),(b,j) \in \mathbb{Z}$. The heuristic expression for $\hat{g}_{ab}^{(n+1)}(ij)$ given by (23) and (24) provides a numerically stable estimator for the transition matrix and allows a more aggressive weighting sequence $\{\gamma_n\}$ to be chosen in the recursive procedure (8) to achieve faster convergence. In our implementation, we set $\gamma_n = \gamma_0 n^{-\varepsilon}$, where $\gamma_0 = 0.3$ and $\varepsilon = 0.35$. Note that in our approach, the projection operator $\Pi_{\mathcal{G}}$ appearing in (8) depends on $\hat{\phi}_n$. In our numerical studies, we have found that computing estimates of all components of the transition matrix G via (8) and then normalizing, as in (23), results in significantly better performance than computing estimates of only the independent components of G. This provides a practical justification for retaining the entire transition matrix as part of the HBMM parameter.

TABLE I
Estimates of HBMM Parameter Components for the Observable Process

	true	Baum	$r = 1$	$r = 2$	$r = 5$
$\hat{\mu}_1$	-112.40	-112.38	-112.49	-112.50	-112.43
$\hat{\sigma}_1$	3.77	3.79	3.75	3.73	3.74
$\hat{\mu}_2$	-45.61	-45.67	-45.62	-45.57	-45.62
$\hat{\sigma}_2$	1.77	1.77	1.78	1.76	1.77

B. Simulation Setup

For our spectrum sensing simulations, the true parameter ϕ^0 of the HBMM was the one used in [24]. That parameter was estimated from real spectrum measurements of a paging channel collected in [26] using the Baum algorithm. The 20×20 transition matrix of that parameter may be found in [22]. The parameter components for the conditionally normal distributions are given in Table I. This HBMM parameter was used to generate the ground truth observation sequence in most of our numerical experiments.

We varied the order r of the HBMM estimate, as well as the length T of the observation sequence generated by the true parameter. We set the initial parameter ϕ^s using a randomly generated transition matrix G^s. In our simulation experiments, the initial values of the HBMM parameter components associated with the conditionally Gaussian observable sequence are given by $(\mu_1^s, \sigma_1^s) = (-120,\ 1)$ and $(\mu_2^s, \sigma_2^s) = (-80,\ 2.24)$. The choice of the order r involves a tradeoff among model accuracy, computational efficiency, and the number of observation samples required to obtain a "good" estimate. Choosing a larger value of r generally requires more observation samples and computation, but can potentially result in better estimates. Estimating the transition matrix G is a much more difficult task than estimating the conditionally normal parameter components. Unless the initial transition matrix G^s is somewhat close to the true transition matrix G, the estimate $\hat{G}$ typically appears to be a rather poor representation of G. Nevertheless, the sojourn time distributions derived from $\hat{G}$ tend to closely approximate the true sojourn time distributions, given a sufficient number of observation samples. For the spectrum sensing application, accuracy of the sojourn time distribution estimates, as obtained from the parameter estimate using (3), is of primary concern, as opposed to convergence of the parameter estimates themselves [24]. Therefore, our results focus on the quality of the estimated sojourn time distributions rather than on convergence of the estimates of the transition matrix.

C. Results

We have tested the recursive parameter estimator developed in this paper, and compared its performance with the Baum algorithm proposed in [22], [24]. We have run the Baum algorithm on $T = 2000$ observations using a predetermined fixed number of iterations. This number was determined by the ratio of the total number of observations available to the recursive algorithm, and $T = 2000$. This approach allows us to compare the two estimators using effectively the same number of observations. For $r = 1$, 2, and 5, the number of Baum iterations was set to 5, 10, and 25, respectively.

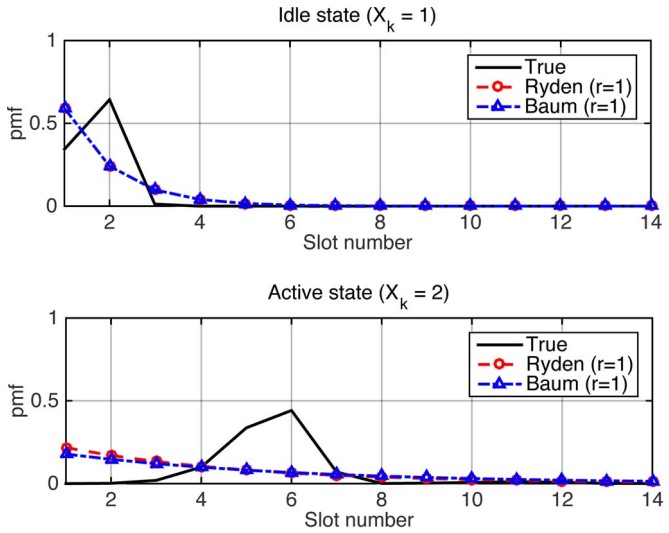

Fig. 1. Estimated sojourn time distributions, $r = 1$ (HMM).

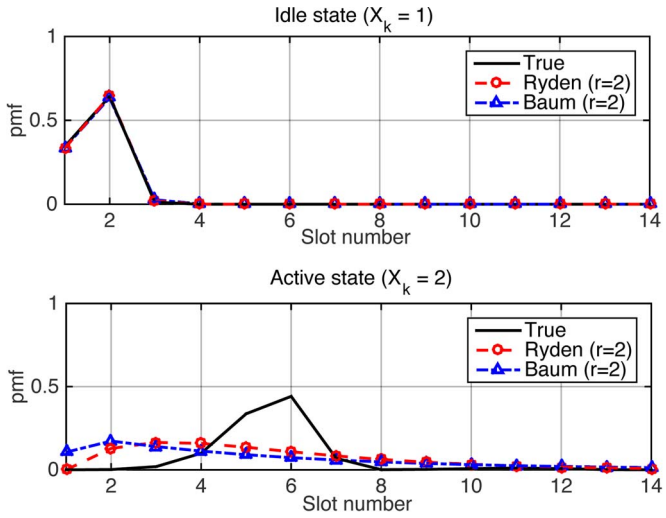

Fig. 2. Estimated sojourn time distributions, $r = 2$.

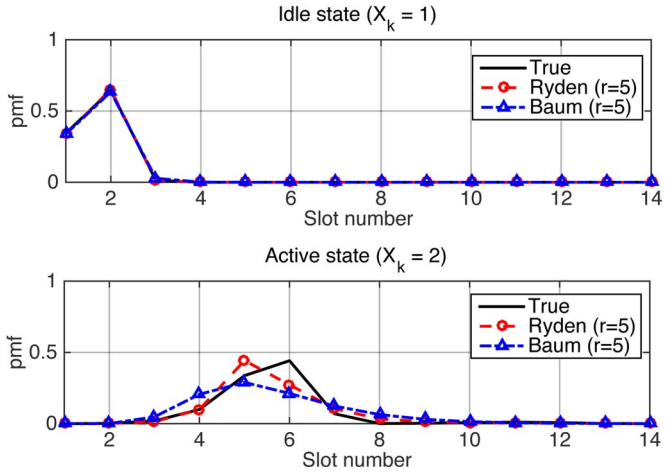

Fig. 3. Estimated sojourn time distributions, $r = 5$.

The estimated values of the components of the parameter which correspond to the conditional Gaussian distributions, as obtained by the Baum algorithm, are shown in Table I in the column labelled 'Baum'. We ran the online algorithm for the same values of $r = 1$, 2, 5 with observation sequence lengths of 10 000, 20 000, and 50 000, respectively. The estimates of (μ_a, σ_a) in this case are given in the columns marked $r = 1$, $r = 2$, and $r = 5$, respectively, in Table I. In all cases, the estimates were very close to the true parameter values. These results underscore the relative ease with which the conditionally Gaussian parameter components can be estimated.

Estimation of the transition matrix of the true model of order $r = 10$, by either the recursive algorithm or the Baum algorithm, has proven to be a much harder task. Our numerical work suggests that for smaller order r of the true parameter, e.g., $r = 2$, 3, both algorithms often converge to an estimate close to ϕ^0, but this is not the case for higher orders. For the spectrum sensing application, however, the accuracy of the estimates is measured by their ability to represent the sojourn times in the active and idle states. Both the recursive and the Baum algorithms provided accurate estimates in this respect for higher model orders of the true parameter, in particular, for $r = 10$.

The sojourn time distributions associated with the estimates of G obtained by applying the online and Baum algorithms for $r = 1$, 2, 5 are shown in Figs. 1, 2, and 3, respectively. For a given parameter estimate, the associated sojourn time distribution is given by (3). When $r = 1$, i.e., when the HBMM is an HMM, the estimated idle $(X_k = 1)$ and active $(X_k = 2)$ state sojourn time distributions appear to be very different from the true ones. The online and Baum algorithms seem to perform similarly in this case. For $r = 2$, the estimated idle state sojourn time distributions obtained using the two algorithms lines up very closely with the true distribution. For the active state distribution, the estimates obtained using the online and Baum algorithms are still far from the true distribution, but some improvement can be observed relative to the case $r = 1$. Significant improvement in the active state sojourn time distribution estimate can be seen when $r = 5$. In this case, the online estimate is superior to the Baum estimate. We note that by increasing the number of iterations, the Baum algorithm will eventually obtain an estimated sojourn time distribution which closely matches that obtained by the online algorithm (cf. Fig. 8 in [24]). To converge in this sense, the Baum algorithm required 15 iterations when $r = 2$ and 50 iterations when $r = 5$.

The recursive algorithm can also be applied repeatedly to a fixed observation sequence in an offline setup similar to that of the Baum algorithm. We applied this alternative offline algorithm, which we refer to as 'online-rep,' to a sequence of $T = 2000$ observation samples and 10 and 25 iterations for model orders of $r = 2$ and 5, respectively. This is equivalent to applying the online algorithm to observation sequences of lengths 20 000 and 50 000, obtained by concatenating the same sequence of 2000 observation samples 10 and 25 times, respectively. We found that the accuracy of the sojourn time distribution estimates obtained using "online-rep" was very similar to that obtained by applying the online algorithm to sequences of length 20 000 and 50 000 generated, respectively, using the true parameter. Fig. 4 compares the estimated sojourn time distributions obtained using "online-rep" vs. those obtained using the online algorithm (labelled "online" as before). The two sojourn time distributions are very close to each

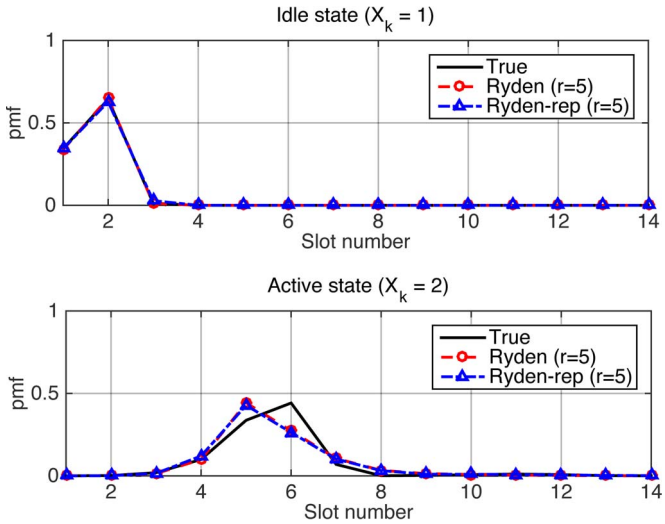

Fig. 4. Estimated sojourn time distributions, $r = 5$.

other and both are more accurate than the estimated sojourn time distributions obtained using an equivalent application of the Baum algorithm (see Fig. 3). Relative to the 'online-rep' algorithm, the Baum algorithm required 50% more iterations when $r = 2$ and 200% more iterations when $r = 5$ to obtain the converged sojourn time distribution estimates.

An important advantage of the online parameter estimator relative to the Baum algorithm is that it can adapt to changes in the true parameter. To demonstrate this feature, we created an observation sequence consisting of 80 000 samples generated using of the true parameter of order $r = 10$ as above, followed by 80 000 samples generated using a different HBMM parameter of order $r = 3$. The sojourn time distributions in the idle and active states of the second HBMM were identical. Consequently, the PU is in the idle and active states with equal probability, which makes state estimation and prediction more difficult in the case of the second HBMM model, relative to the first.

The recursive state prediction scheme (6) together with the online parameter estimator (8), using an HBMM of order $r = 5$ and with $\eta = 0.5$, were applied to the concatenated observation sequence of 160 000 samples, The observation sequence was divided into 80 groups of 2000 samples each. Fig. 5 shows the real-time τ-step state prediction performance ($\tau = 1$, 3, 6, 9) of the spectrum sensing scheme. The horizontal axis indicates the group number, while the vertical axis represents the error probability of the prediction scheme (6), $P_{\rm pe}$, computed by averaging over each group of 2000 observation samples. The online parameter estimator is initialized with a randomly chosen initial parameter. At group number 40, the model changes to the second HBMM parameter and a spike in $P_{\rm pe}$, as expected, can be observed for all values of τ. For $\tau = 1$, the error probability drops quickly at group 41 and reaches a steady-state level of about 0.18 after an additional 2–3 groups of observation samples. For the other values of τ, the error performance takes 1–2 additional groups of observation samples to attain steady-state. To summarize, the error performance of the state prediction scheme required fewer than 6000 observation samples to converge to steady-state. On the other hand, as noted earlier, for

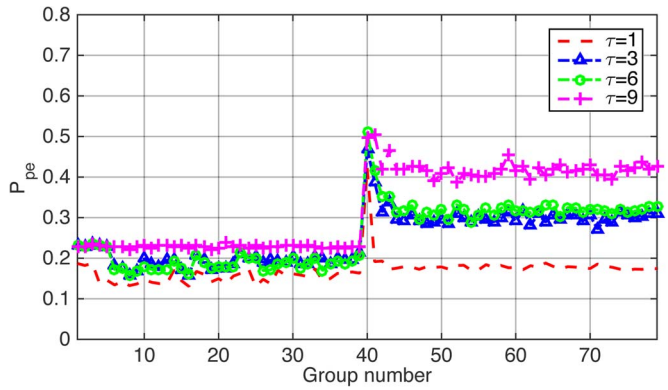

Fig. 5. τ-step error probability for the state prediction scheme ($r = 5, \eta = 0.5$) vs. observation group number.

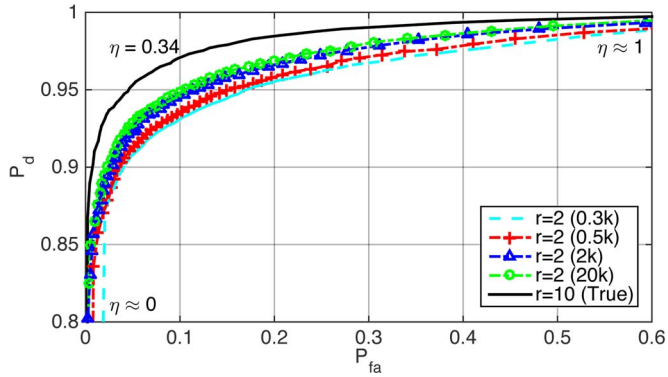

Fig. 6. ROC plot, $r = 2$.

the same order $r = 5$, about 50 000 observation samples were required for the sojourn time distribution estimates to converge. Thus, the error performance of the state prediction scheme converges much faster than the sojourn time distribution estimates.

To gain further insight into the performance of the proposed online spectrum sensing scheme, we consider the ROC performance of the state estimator given by (6) when $\tau = 0$. We use an HBMM parameter with the same transition matrix G for $r = 10$ as before, but the parameters of the observable process are modified to reflect a more prominent shadowing effect in the wireless channel as in [24, Eq. (26)], as follows:

$$(\mu_1, \sigma_1) = (-112.40, 3.77),\ (\mu_2, \sigma_2) = (-95.40, 8.19). \quad (25)$$

To obtain a ROC curve, we simulate a set of sample paths of an HBMM characterized by the true parameter ϕ^0. For each sample path, the online parameter estimator (8) and the state detection scheme in (6), with a fixed detection threshold η, are applied. The false alarm and missed detection probabilities corresponding to the fixed value of η are computed by averaging over the set of samples paths. This procedure is repeated for values of η in the interval (0, 1) to obtain the ROC curve.

Fig. 6 shows a family of ROC curves for parameter estimates of order $r = 2$ obtained by applying the online procedure to observation sequences of length 300, 500, 2000, and 20 000 (labelled 0.3k, 0.5k, 2k, and 20k, respectively), which were generated using the modified HBMM parameter of order $r = 10$. For a given parameter estimate, an ROC curve was obtained

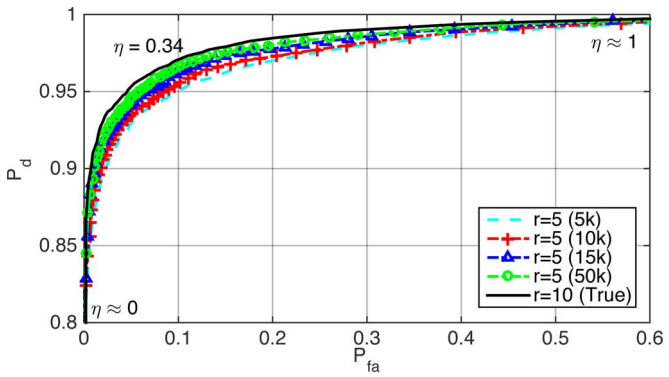

Fig. 7. ROC plot, $r = 5$.

by applying the state estimator in (6) with each new observation group of length 20 000. Observe that the parameter estimates labelled 2k and 20k have similar ROC performance. We also see that the ROC curves labelled 0.3k and 0.5k are close to each other, while not being significantly far from the 2k curve. These results suggest that it is not necessary for the sojourn time distribution estimates to converge to achieve good ROC performance; i.e., given a relatively small number of observation samples, the online estimator yields estimates with acceptable ROC performance. We remark that the ROC plots in Figs. 6 and 7 are relatively insensitive to the choice of initial parameter for the estimators.

Fig. 7 shows a family of ROC curves obtained using parameter estimates of order $r = 5$. In this case, five parameter estimates were obtained using observation sequences of length 5000, 10 000, 15 000, and 50 000 (labelled 5k, 10k, 15k, and 50k, respectively). All of these curves show superior performance relative to the order $r = 2$ estimates from Fig. 6. On the other hand, more observation samples are generally needed to obtain good parameter estimates for higher values of the model order r. There is a clear gap between the 5k and 50k curves, but the difference between the curves is relatively small. This again suggests that even with a relatively small number of observation samples, the online parameter estimator provides parameter estimates, which in combination with the recursive state estimation scheme, result in good ROC performance.

V. Conclusion

We developed a computationally efficient online algorithm for estimating the parameter of an HBMM for temporal spectrum sensing. The proposed algorithm is based on a block-recursive parameter estimator for HMMs developed by Rydén [25]. Rydén's algorithm was supplemented with an efficient recursion to compute the score function. That recursion was developed along the lines of a similar recursion for the score function of an MMPP by Willy *et al.* [32]. The online parameter estimator is able to adapt to changes in the true parameter and, in combination with the recursive state estimation and prediction scheme proposed in [24], provides an effective scheme for online temporal spectrum sensing. An alternative recursive procedure for estimating the parameter of an HBMM, which does not involve computation of the score function, is developed in [6].

We focused on temporal sensing for a narrowband channel with lognormal shadowing, based on received signal strength measurements. It would be of interest to consider applying the HBMM-based spectrum sensing approach in multichannel scenarios (cf. [30]) and with different channel models or receiver front-ends. To cope with severely shadowed environments, the proposed sensing approach could be extended to a cooperative setup involving multiple cognitive radios (cf. [16], [31]). The temporal sensing approach proposed here could also be combined with spatial sensing to further increase spectrum utilization (cf. [4]).

Acknowledgment

We thank Tobias Rydén for his valuable help in the implementation process of his recursive parameter estimation algorithm. We also thank the anonymous reviewers for their constructive comments, which have helped us to improve the presentation of the paper.

References

[1] I. A. Akbar and W. H. Tranter, "Dynamic spectrum allocation in cognitive radio using hidden Markov models: Poisson distributed case," in *Proc. IEEE SoutheastCon*, Mar. 2007, pp. 196–201.

[2] L. E. Baum and T. Petrie, "Statistical inference for probabilistic functions of finite state Markov chains," *Annals Math. Statist.*, vol. 37, no. 6, pp. 1554–1563, Apr. 1966.

[3] A. P. Dempster, N. M. Laird, and D. B. Rubin, "Maximum likelihood from incomplete data via the EM algorithm," *J. R. Statist. Soc.*, vol. 39, no. 1, pp. 1–38, 1977.

[4] T. Do and B. L. Mark, "Joint spatial-temporal spectrum sensing for cognitive radio networks," *IEEE Trans. Veh. Technol.*, vol. 59, no. 7, pp. 3480–3490, Sep. 2010.

[5] Y. Ephraim and B. L. Mark, "Bivariate Markov processes and their estimation," *Found. Trends Signal Process.*, vol. 6, no. 1, pp. 1–95, Jun. 2013.

[6] Y. Ephraim and B. L. Mark, "Causal recursive parameter estimation for discrete-time hidden bivariate Markov chains," *IEEE Trans. Signal Process.*, vol. 63, no. 8, pp. 2108–2117, Apr. 2015.

[7] Y. Ephraim and N. Merhav, "Hidden Markov processes," *IEEE Trans. Inf. Theory*, vol. 48, no. 6, pp. 1518–1569, Jun. 2002.

[8] FCC, "Spectrum policy task force," Fed. Commun. Comm., Washington, DC, USA, Tech. Rep. 02-135, Nov. 2002.

[9] S. Geirhofer, L. Tong, and B. M. Sadler, "Dynamic spectrum access in the time domain: Modeling and exploiting white space," *IEEE Commun. Mag.*, vol. 45, no. 5, pp. 66–72, May 2007.

[10] C. Ghosh, C. Cordeiro, D. P. Agrawal, and M. B. Rao, "Markov chain existence and hidden Markov models in spectrum sensing," in *Proc. IEEE Int. Conf. PerCom*, Mar. 2009, pp. 1–6.

[11] K. Haghighi, E. G. Ström, and E. Agrell, "On optimum causal cognitive spectrum reutilization strategy," *IEEE J. Sel. Areas Commun.*, vol. 30, no. 10, pp. 1911–1921, Nov. 2012.

[12] U. Holst and G. Lindgren, "Recursive estimation in mixture models with Markov regime," *IEEE Trans. Inf. Theory*, vol. 37, no. 6, pp. 1683–1690, Nov. 1991.

[13] V. Krishnamurthy and J. Moore, "On-line estimation of hidden Markov model parameters based on the Kullback-Leibler information measure," *IEEE Trans. Signal Process.*, vol. 41, no. 8, pp. 2557–2573, Aug. 1993.

[14] P. Lanchantin, J. Lapuyade-Lahorgue, and W. Pieczynski, "Unsupervised segmentation of randomly switching data hidden with non-Gaussian correlated noise," *Signal Process.*, vol. 91, no. 2, pp. 163–175, Feb. 2011.

[15] G. Latouche and V. Ramaswami, *Introduction to Matrix Analytic Methods in Stochastic Modeling*, ser. ASA/SIAM Series on Statistics and Applied Probability. Philadelphia, PA, USA: Soc. Ind. Appl. Math., 1999.

[16] A. E. Leu, M. McHenry, and B. L. Mark, "Modeling and analysis of interference in Listen-Before-Talk spectrum access schemes," *Int. J. Netw. Manag.*, vol. 16, pp. 131–141, Mar. 2006.

[17] B. Li, C. Zhao, M. Sun, Z. Zhou, and A. Nallanathan, "Spectrum sensing for cognitive radios in time-variant flat fading channels: A joint estimation approach," *IEEE Trans. Commun.*, vol. 62, no. 8, pp. 2665–2680, Aug. 2014.
[18] B. L. Mark and A. E. Leu, "Local averaging for fast handoffs in cellular networks," *IEEE Trans. Wireless Commun.*, vol. 6, no. 3, pp. 866–874, Mar. 2007.
[19] B. L. Mark and A. O. Nasif, "Estimation of maximum interference-free transmit power level for opportunistic spectrum access," *IEEE Trans. Wireless Commun.*, vol. 8, no. 5, pp. 2505–2513, May 2009.
[20] J. W. Mark and W. Zhuang, *Wireless Communications and Networking*. New York, NY, USA: Pearson Education, Inc., 2003.
[21] M. F. Neuts, *Matrix-Geometric Solutions in Stochastic Models*. Baltimore, MD, USA: The Johns Hopkins Univ. Press, 1981.
[22] T. Nguyen, "Hidden Markov model based spectrum sensing for cognitive radio," PhD dissertation, Dept. Electr. Comput. Eng., George Mason Univ., Apr. 2013.
[23] T. Nguyen, B. L. Mark, and Y. Ephraim, "Hidden Markov process based dynamic spectrum access for cognitive radio," in *Proc. CISS*, Baltimore, MD, USA, Mar. 2011, pp. 1–6.
[24] T. Nguyen, B. L. Mark, and Y. Ephraim, "Spectrum sensing using a hidden bivariate Markov model," *IEEE Trans. Wireless Commun.*, vol. 12, no. 9, pp. 4582–4591, Aug. 2013.
[25] T. Rydén, "On recursive estimation for hidden Markov models," *Stochastic Process. Appl.*, vol. 66, no. 1, pp. 79–96, Feb. 1997.
[26] "General survey of radio frequency bands: 30 MHz to 3 GHz," Shared Spectrum Comp., Vienna, VA, USA, Tech. Rep., Aug. 2010.
[27] Y. Sun and B. L. Mark, "Interference model for spectrum sensing with power control," in *Proc. CISS*, Baltimore, MD, USA, Mar. 2013, pp. 1–6.
[28] Z. Sun, G. Bradford, and N. Laneman, "Sequence detection algorithms for PHY-layer sensing in dynamic spectrum access networks," *IEEE J. Sel. Topics Signal. Process.*, vol. 5, no. 1, pp. 97–109, Feb. 2011.
[29] K. W. Sung, S.-L. Kim, and J. Zander, "Temporal spectrum sharing based on primary user activity prediction," *IEEE Trans. Wireless Commun.*, vol. 9, no. 12, pp. 3848–3855, Dec. 2010.
[30] P. Tehrani, L. Tong, and Q. Zhao, "Asymptotically efficient multichannel estimation for opportunistic spectrum access," *IEEE Trans. Signal Process.*, vol. 60, no. 10, pp. 5347–5360, Oct. 2012.
[31] J. Unnikrishnan and V. Veeravalli, "Cooperative sensing for primary detection in cognitive radio," *IEEE J. Sel. Topics Signal. Process.*, vol. 2, no. 1, pp. 18–27, Feb. 2008.
[32] C. J. Willy, W. J. J. Roberts, and T. A. Mazzuchi, "Recursions for the MMPP score vector and observed information matrix," *Stochastic Models*, vol. 26, no. 4, pp. 649–665, Jul. 2010.
[33] S. Z. Yu, "Hidden semi-Markov models," *Artif. Intell.*, vol. 174, no. 2, pp. 215–243, Feb. 2010.
[34] T. Yucek and H. Arslan, "A survey of spectrum sensing algorithms for cognitive radio applications," *IEEE Commun. Surveys Tuts.*, vol. 11, no. 1, pp. 116–130, Mar. 2009.

Yuandao Sun (S'15) received the B.S. degree in electronics and information engineering from Zhejiang Gongshang University, Hangzhou, China, and the M.S. degree in electrical and computer engineering from Tongji University, Shanghai, China. He is currently pursuing the Ph.D. degree in electrical and computer engineering at George Mason University, Fairfax, VA, USA. His current research interests include wireless communications, signal processing, and cognitive radio technology.

Brian L. Mark (S'91–M'95–SM'08) received the Ph.D. degree in electrical engineering from Princeton University, in 1995, and the B.A.Sc. degree in Computer Engineering with an option in Mathematics from the University of Waterloo, in 1991. He was a Research Staff Member at C&C Research Laboratories, NEC USA, from 1995 to 1999. In 1999, he was on part-time leave from NEC as a Visiting Researcher at Ecole Nationale Supérieure des Télécommunications, Paris, France. In 2000, he joined George Mason University, where he is currently Professor of Electrical and Computer Engineering. His research interests lie in the design and performance analysis of communication networks. He served as an associate editor for IEEE TRANSACTIONS ON VEHICULAR TECHNOLOGY from 2006–2009.

Yariv Ephraim (S'82–M'84–SM'90–F'94) received the D.Sc. degree in electrical engineering from the Technion-Israel Institute of Technology, Haifa, Israel, in 1984. During 1984–1985, he was a Rothschild Post-Doctoral Fellow at the Information Systems Laboratory, Stanford University, Palo Alto, CA, USA. During 1985–1993, he was a Member of Technical Staff at the Information Principles Research Laboratory, AT&T Bell Labs, Murray Hill, NJ, USA. In 1991, he joined George Mason University, Fairfax, VA, USA, where he currently is Professor of Electrical and Computer Engineering. His research interests are in statistical signal processing.